

Additional considerations about the role of ion size in charge reversal

This article has been downloaded from IOPscience. Please scroll down to see the full text article.

2009 J. Phys.: Condens. Matter 21 424105

(<http://iopscience.iop.org/0953-8984/21/42/424105>)

View [the table of contents for this issue](#), or go to the [journal homepage](#) for more

Download details:

IP Address: 129.252.86.83

The article was downloaded on 30/05/2010 at 05:34

Please note that [terms and conditions apply](#).

Additional considerations about the role of ion size in charge reversal

A Martín-Molina^{1,3}, R Hidalgo-Álvarez¹ and M Quesada-Pérez²

¹ Grupo de Física de Fluidos y Biocoloides, Departamento de Física Aplicada, Facultad de Ciencias, Universidad de Granada, Granada 18071, Spain

² Departamento de Física, Universidad de Jaén, Escuela Politécnica Superior de Linares, 23700 Linares, Jaén, Spain

E-mail: almartin@ugr.es

Received 30 March 2009, in final form 29 April 2009

Published 29 September 2009

Online at stacks.iop.org/JPhysCM/21/424105

Abstract

The effect of the ion size on the charge reversal process is studied via canonical Monte Carlo simulation. To this end, a primitive model of electrolyte is used to analyze the electric double layer formed by an asymmetric electrolyte in the presence of a charged planar wall. Different values of ion diameters and surface charge densities are used so as to determine the conditions at which the charge reversal first occurs. For each case, the apparent surface charge density is calculated as a function of the distance from the charged wall for the different electrolyte concentrations in order to establish the minimal salt concentration required for the charge reversal. We will refer to this electrolyte concentration as the *reversal concentration* and will show how it depends on the surface charge density and on the ion size. From the apparent surface charge density profiles, the distance from the wall at which the charge reversal arises as well as its intensity can be also inferred.

(Some figures in this article are in colour only in the electronic version)

1. Introduction

The ion distribution around a charged surface immersed in an electrolytic solution is termed an electric double layer (EDL). Obviously, these ionic structures govern the electrostatic interactions of the charged particles and therefore they play an essential role in the stability and electrokinetic behavior of colloidal dispersions. As a consequence, it is of crucial importance to choose an appropriate model to describe such ion distribution. According to Grochowski and Trylska, the EDL models are classified into two groups: *explicit solvent models* and *implicit solvent models* [1]. In the former the solvent molecules are explicitly considered, thus an enormous number of computational calculations are required to model the electrostatic interactions. In contrast, implicit solvent models use a mean field approach to treat the solution as a continuum where the ions are immersed. This is the case of the classical Gouy–Chapman (GC) model, in which the colloidal particles are smooth and uniformly charged planes immersed in a dielectric continuum comprised of mobile ions. Although this

model has been extensively used to describe the colloidal EDL, its applicability is restricted to systems where the concentration of (mostly monovalent) electrolyte and the surface charge are low. Apart from these situations, the theory is defective mainly because it is based on the conventional Poisson–Boltzmann (PB) equation in which the ions are considered as point charges. Failures of the classical approach have been corroborated by a large variety of simulations and sophisticated models in which the ion size has been implemented in different ways (see the revision works [1–6]). The overlooking of the phenomenon generally known as *charge reversal* is probably one of the most representative examples of the breakdown of the classical approach. Charge reversal is referred as the excessive compensation of the native colloidal charge, prompted by strongly attracted counterions, leading to an effective macroparticle charge of reversed sign [7]. In the last decades this phenomenon has become particularly important because it is responsible for a number of phase transitions in biocolloidal systems involving DNA [8–10]. As a consequence of its importance, charge reversal has recently captured the attention of numerous theoretical scientists interested in the origin of such an effect. According to Pianegonda *et al*, the

³ Author to whom any correspondence should be addressed.

clue to the mechanism of charge reversal is that the PB equation fails to account for its existence [11]. Since this mean field theory neglects the ion correlations derived from their finite size, such correlations could be responsible (at least partly) for the charge reversal. Thus a vast number of theories that take into account ionic correlations have been recently developed to establish the mechanism of charge reversal. For instance, many works have been devoted to modify the PB equation in order to include the finite ion size in the calculations ([1, 12] and references cited therein). Alternatively, theories based on integral equations [4, 7], field-theoretic approaches [13, 14], density functional theories [15, 16], and one component plasma (OCP) models have been also put forward to describe the colloidal charge reversal [3, 11, 17]. Unfortunately, none of the theories can fully account for the experimental findings (see for instance [18]). Moreover, neither are all the models analytical nor do they agree in their conclusions. In view of this, computer simulations are frequently used to study the validity of the theoretical models and they have even been used as alternative methods to the theoretical models [16, 19–33].

On the other hand, due to the increasing interest of experimentalists in using the charge reversal theories with analytical solutions, the OCP models developed by Shklovskii, Levin and their respective co-workers appear as the most popular theories [3, 11, 17]. According to such approaches, the multivalent ionic atmosphere confined at the macroion surface is approximated by a two-dimensional Wigner crystal (WC). This kind of model is widely used in the literature since they present quite simple equations to describe the EDL of macroions with different geometries in the presence of multivalent ions. In this sense, charge reversal of colloids, membranes, DNA molecules, etc, are straightforwardly predicted in terms of these expressions [10, 34, 35]. Although under certain conditions (such as the case of a mixture of electrolytes) simulations and theories do not always agree, the predictions obtained from these models in the strong-coupling regime are in general consistent with simulations [29, 32]. In this regime, the intensity of the ionic electrostatic correlations is strong enough to form WC-like structures. This situation occurs for large values of the so-called *coupling parameter*, Γ , that strongly depends on the colloidal charge [29].

Although the OCP models could successfully describe the mechanism for charge reversal in the strong-coupling limit ($\Gamma \gg 1$), the situation is not so clear for weak electrostatic coupling. For this reason, the role of ion size in this phenomenon has been extensively studied from simulations in many of our previous works [18, 23, 24, 28, 33, 36]. Recently, Diehl and Levin have also studied the effect of ion size on the critical colloidal surface charge density (σ_c) at which charge reversal first appears via MC simulations [37]. These authors calculated the ζ -potential as a function of the surface charge density (σ_0) for a high concentration of 3:1 electrolyte (0.1 M) in order to predict the value of σ_0 at which the electrophoretic mobility reversal first takes place. They proved that this critical value depends strongly on the ionic size and showed how σ_c depends on the salt concentration for two electrolytes, 3:1 and 2:1, by using as ionic radii (a) 0.2 and 0.3 nm, respectively. In general, σ_c exhibited an inflection point, which is a function of

the salt concentration. The maximum value of σ_0 studied was 0.08 C m^{-2} . In any case it should be stressed that these authors calculated the ζ -potential at a distance of one ionic diameter from the surface (instead of an ionic radius), which had been justified in a previous work [38]. According to Diehl and Levin, the traditional location of the shear plane has a serious shortcoming that is overcome with this assumption: the ζ -potential strongly depends on any small perturbation since the variation of the electrostatic potential is very rapid at distances of about one ionic radius.

In the same spirit, we have made a systematic study of the minimal 3:1 salt concentration at which charge reversal first occurs (reversal concentration), for different ionic radii and σ_0 values. To this end, we simulate a planar EDL by using a restrictive primitive model of electrolyte. In particular, given a value of σ_0 and a , our simulations provide an apparent surface charge density as a function of the distance from the charged wall for different electrolyte concentrations. From these profiles, the reversal concentrations are estimated for each case. Similarly to the work of Diehl and Levin, the effect of the ionic size on charge reversal is studied. However, some differences must be also stressed.

- (i) Our results are expressed in terms of a critical electrolyte concentration instead of a critical surface charge density reversal.
- (ii) Our estimates of the reversal concentrations are based on the profiles of the apparent surface charge density (defined later) instead of the change of sign of the ζ -potential. In this way, such values do not depend on the location of the shear plane and this long-standing question is avoided (as well as the inconveniences of the rapid variation of the electrostatic potential near the charged surface).
- (iii) We use ranges of σ_0 and a larger than those employed by the cited work. In particular, the maximum value of σ_0 studied is (in magnitude) 0.14 C m^{-2} , whereas the ionic radii chosen are 0.2 and 0.4 nm. In our opinion, these conditions are more consistent with the experimental conditions studied in our previous works [18, 39] and the hydrated ion sizes found in the scientific literature [40].

2. Model and simulations

Our simulations have been carried out in the framework of the restricted primitive model, in which small ions are treated as charged hard spheres of the same size immersed in a dielectric continuum (water at 298 K in this case). According to this EDL representation, the interaction energy between ions i and j is given by

$$u(\vec{r}_{ij}) = \begin{cases} \frac{Z_i Z_j e^2}{4\pi \epsilon_0 \epsilon_r r_{ij}} & r_{ij} \geq d \\ \infty & r_{ij} < d \end{cases} \quad (1)$$

where $d = 2a$ is the hydrated ion diameter, ϵ_0 is the permittivity of vacuum, $\epsilon_r = 78.5$ is the relative permittivity, \vec{r}_{ij} is the relative position vector and $r_{ij} = |\vec{r}_{ij}|$ is the distance between ions i and j . Restricting ourselves to the case of a

planar EDL, a uniformly charged plane wall is located at $z = 0$. Another impenetrable wall without charge is placed at $z = L$. The interaction energy of ion i with the charged wall is given by

$$u(\vec{r}_i) = \begin{cases} -\frac{\sigma_0 Z_i e z_i}{2\epsilon_0 \epsilon_r} & z_i \geq d/2 \\ \infty & z_i < d/2 \end{cases} \quad (2)$$

where z_i is the z -coordinate of particle i and σ_0 is the surface charge density of the charged wall.

Some technical aspects of the computer simulations for a planar EDL in the presence of a charged wall deserve to be briefly commented on. The Metropolis algorithm was applied to a canonical ensemble for a collection of N ions confined in a rectangular prism (simulation cell) at constant temperature, whose dimensions are $W \times W \times L$. Periodic boundary conditions were used in the lateral directions (x and y). The simulation cell contains the ionic electrolyte mixture corresponding to the bulk solution within a counterion excess neutralizing the surface charge of the charged wall to ensure the whole simulation cell is always neutral. Moreover, the systems were always thermalized before collecting data for averaging and the acceptance ratio was kept between 0.3 and 0.5. Due to the long range of the electrostatic interactions, the energy must be evaluated very carefully. In this work, the so-called Lekner–Sperb method was applied (see [18, 23, 24, 29, 33, 36] for further details). The values of W , L and N are quite similar to those employed in previous papers where the Lekner–Sperb method was also used.

In this work we will restrict ourselves, as a preliminary survey, to the case of electrolytes with trivalent counterions and monovalent coions (3:1), since these electrolytes have been widely investigated both theoretical and experimentally. On one hand, according to the OCP models the electrostatic interactions between trivalent counterions are strong enough to form a strong correlated structure liquid on the macroion surface, which would justify the appearance of charge reversal in these systems [3, 11, 17]. On the other hand, mobility reversals have been reported for four decades in the presence of 3:1 electrolytes [18, 41, 42].

3. Results and discussion

Nowadays it is widely known that the charge reversal can be revealed through different physical properties. In most of our previous works, we have focused on the diffuse potential because this quantity is intimately related to measurable electrokinetic properties, such as the electrophoretic mobility (μ_e) [18, 23, 24, 28, 33, 36]. Both ψ_d and μ_e undergo sign reversals that are somehow associated with the phenomenon of charge reversal. Due to its definition, however, the diffuse potential is strongly influenced by ion size. This might be a serious shortcoming to discriminate ion size correlations from other size effects when two or more series of data corresponding to different ionic diameters are compared.

For this reason (and other advantages previously commented on), the effect of ion size on charge reversal will be analyzed in this work from another physical quantity,

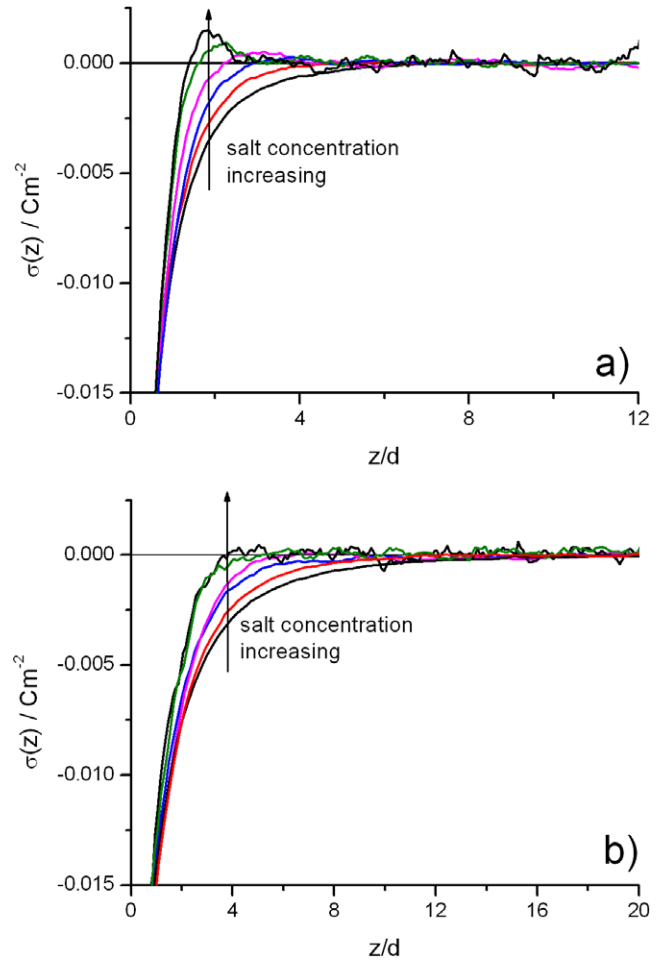


Figure 1. Integrated surface charge density, $\sigma(z)$, for $\sigma_0 = -0.02 \text{ C m}^{-2}$ and (a) $d = 0.8 \text{ nm}$ and 3:1 electrolyte concentrations of 5, 10, 20, 40, 80 and 120 mM; (b) $d = 0.4 \text{ nm}$ and the same electrolyte concentrations. The electrolyte concentration increases from bottom to top (see the arrow).

the apparent surface charge density, which is mathematically defined as follows:

$$\sigma(z) = \sigma_0 + \int_0^z \sum_i \rho_i(z) dz \quad (3)$$

where ρ_i is the local concentration of species i . $\sigma(z)$ plays a fundamental role in the EDL theory and represents the total (or integrated) charge in a column of liquid of unit cross section extending from the surface to a plane located at z [43]. In other words, $\sigma(z)$ is the surface charge density *seen* from a distance z to the charged surface. This or similar definitions have been employed in previous studies of charge reversal [44–46]. In any case, the definition of $\sigma(z)$ is obviously based on the concept of charge and does not involve ion size directly. Consequently, the variations observed in changing the ionic diameter can be unequivocally attributed to ion size correlations.

First, we will discuss the results corresponding to a surface charge density $\sigma_0 = -0.02 \text{ C m}^{-2}$ and an ionic diameter of 0.8 nm. In figure 1(a), we have plotted this function for different 3:1 electrolyte concentrations. For 5 and 10 mM,

$\sigma(z)$ is clearly a monotonic function, whose absolute value decreases from $-\sigma_0$ (at the outer Helmholtz plane) to 0 (at the bulk of the solution). Mathematically speaking, the monotony is a well established feature in the PB description of the EDL since other properties are also characterized by a monotonic behavior in such an approach, such as the ionic profiles or the electrostatic potential [4]. However, for higher salt concentrations, the monotonicity of $\sigma(z)$ disappears. For 20 mM, this function seems to show small positive values. This behavior is clearly observed for 40 mM. What is more, $\sigma(z)$ now exhibits a maximum around $z \approx 3d$, which is a clear signal of charge reversal. These two features (positive values for a negatively charged surface and maximum) are confirmed and perfectly observed for 80 mM. In fact, the maximum tends to be more pronounced with increasing salt amount. In any case, one could think that the integrated charge changes its behavior (from monotonic to non-monotonic) at a salt concentration between 10 and 20 mM (let us say 15 mM). In other words, for $\sigma_0 = -0.02 \text{ C m}^{-2}$, the estimated reversal concentration is around 15 mM. In fact, we will define this property as the minimal salt concentration from which $\sigma(z)$ is no longer monotonic but exhibits a maximum (with positive values). Mathematically these features can be revealed from changes of sign in the first derivative of this function. In any case, the value of the reversal concentration will be affected by some uncertainty. Among its sources we mention the statistical fluctuations associated with MC samplings, which can be significant in some cases (as will be illustrated below).

Now we will discuss the results on $\sigma(z)$ for the same surface charge density but a smaller ionic diameter: $d = 0.4 \text{ nm}$. According to previous studies, this diameter is rather small for hydrated trivalent cations. However, the influence of ionic size can be elucidated more easily comparing results for two (or even more) different ion diameters. In figure 1(b), $\sigma(z)$ is again plotted for $\sigma_0 = -0.02 \text{ C m}^{-2}$, but now with $d = 0.4 \text{ nm}$. The comparison between figures 1(a) and (b) reveals a nontrivial difference in the evolution of $\sigma(z)$ with increasing 3:1 electrolyte concentration: the integrated charge does not exhibit a clear maximum with increasing salt amount even up to 120 mM, which represents a high ionic strength for 3:1 electrolytes. In fact, it is not easy to explore much larger salt concentrations in MC simulations. Thus one can only conclude that, if the reversal concentration for 0.4 nm exists, it must be appreciably larger than that obtained for 0.8 nm.

This suggests that, even dealing with trivalent counterions, ion size correlations play an important role in the mechanism of charge reversal if the surface charge density is small. Some authors claim that large surface charge densities enhance electrostatic correlations [3, 17]. In principle, this is logical from a theoretical viewpoint since multivalent counterions in the vicinity of the charged macroion could pack more closely and would enhance electrostatic correlations between them. This aspect can also be discussed with the help of the electrostatic-coupling parameter (for Z-ions), which is defined by Pianegonda *et al* by [11]

$$\Gamma = Z^2 l_B / 2R \quad (4)$$

where l_B is the so-called Bjerrum length and $2R$ is the average separation between multivalent counterions on the macroion

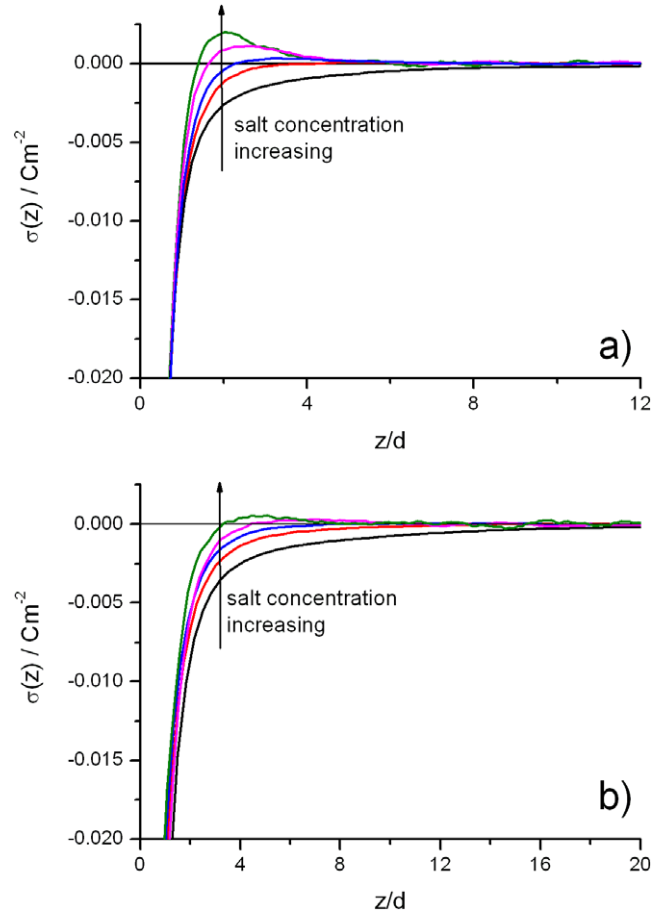


Figure 2. Integrated surface charge density, $\sigma(z)$, for $\sigma_0 = -0.05 \text{ C m}^{-2}$ and (a) $d = 0.8 \text{ nm}$ and 3:1 electrolyte concentrations of 1, 4, 8, 15 and 30 mM; (b) $d = 0.4 \text{ nm}$ and the same electrolyte concentrations. The electrolyte concentration increases from bottom to top (see the arrow).

surface, which can be estimated as $2R = 2\sqrt{Ze/\pi|\sigma_0|}$. It should be kept in mind that this definition differs by a factor of 1/2 from that used by Grosberg *et al* [17]. For trivalent ions and $\sigma_0 = -0.02 \text{ C m}^{-2}$, $\Gamma \approx 1.2$, which is just slightly larger than 1. Consequently, the electrostatic coupling is too weak and would not contribute to charge reversal significantly. However, strong electrostatic correlations are not the only mechanism for this phenomenon. For monovalent ions recent studies have proved that hydrophobic interactions and ionic dispersion forces can induce mobility and diffuse potential reversals [36, 47]. In addition, some authors have reported charge reversal for monovalent ions (and low surface charge density) from simulations [45, 46]. Consequently, the reversal revealed in figure 1(a) for $\sigma_0 = -0.02 \text{ C m}^{-2}$ (and $d = 0.8 \text{ nm}$) could be mostly attributed to ion size correlations. In reducing the ionic diameter ($d = 0.4 \text{ nm}$, figure 1(b)) neither size correlations nor electrostatic interactions would be strong enough to induce reversal.

Now, we will consider the case of a system with a slightly larger surface charge density. In figure 2(a) some $\sigma(z)$ functions corresponding to a surface charge density $\sigma_0 = -0.05 \text{ C m}^{-2}$, $d = 0.8 \text{ nm}$ and different salt concentrations

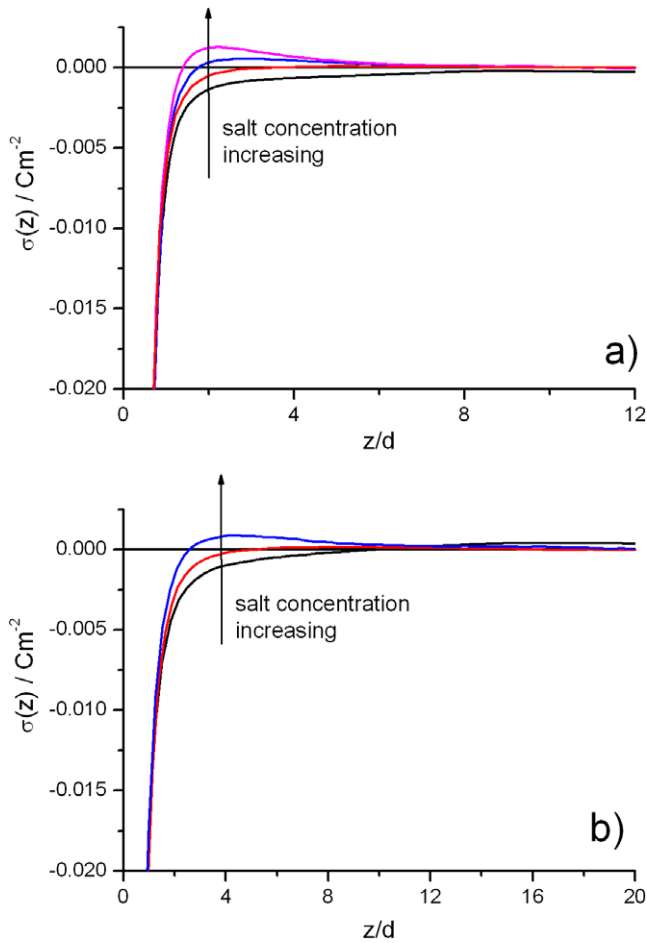


Figure 3. Integrated surface charge density, $\sigma(z)$, for $\sigma_0 = -0.09 \text{ C m}^{-2}$ and (a) $d = 0.8$ nm and 3:1 electrolyte concentrations of 1, 3 and 8 mM; (b) $d = 0.4$ nm and 3:1 electrolyte concentrations of 1, 2, 4 and 8 mM. The electrolyte concentration increases from bottom to top (see the arrow).

are plotted. As can be concluded, the transition to the charge reversal regime is now more evident. In any case, we can also obtain an estimate of the reversal concentration for -0.05 C m^{-2} from figure 2(a). $\sigma(z)$ is not monotonic for salt concentrations larger than 4 mM. Consequently, the reversal concentration should be around this value.

In figure 2(b), the evolution of $\sigma(z)$ with increasing salt concentration is plotted for $\sigma_0 = -0.05 \text{ C m}^{-2}$ and $d = 0.4$ nm. There are two features of this figure that deserve some comments. On the one hand, we conclude after detailed inspection that the reversal concentration is around 8 mM, since larger salt concentrations are required for non-monotonic $\sigma(z)$ functions. This value is a bit larger than that obtained for 0.8 nm. On the other hand, it is worth comparing the maxima of $\sigma(z)$ at 30 mM for $d = 0.8$ and 0.4 nm (figures 2(a) and (b), respectively). As can be easily inferred, the maximum obtained for 0.8 nm is more pronounced than that observed for 0.4 nm. The same conclusion is valid for 15 mM. These differences between both figures can be unequivocally attributed to ion size correlations. Their effect is also important for $\sigma_0 = -0.05 \text{ C m}^{-2}$, although it is much more crucial for $\sigma_0 = -0.02 \text{ C m}^{-2}$, as discussed earlier.

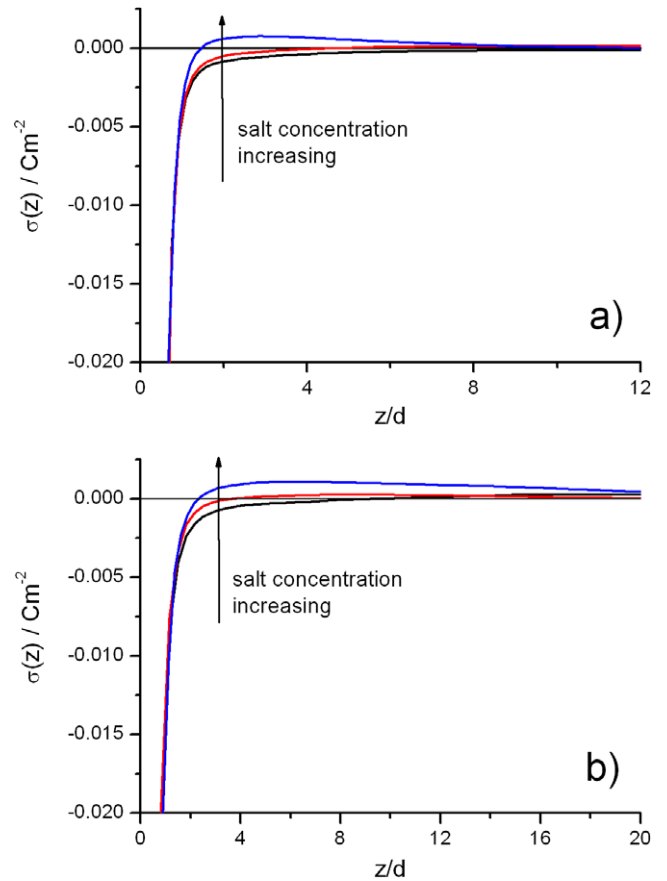


Figure 4. Integrated surface charge density, $\sigma(z)$, for $\sigma_0 = -0.11 \text{ C m}^{-2}$ and (a) $d = 0.8$ nm and 3:1 electrolyte concentrations of 0.5, 1 and 2 mM; (b) $d = 0.4$ nm and the same electrolyte concentrations. The electrolyte concentration increases from bottom to top (see the arrow).

Again, the analysis in terms of Γ can also shed light on this matter. Although their definition of charge reversal is not the same as that applied here, Pianegonda *et al* state that, for trivalent ions and $d = 0.4$ nm, the reversal will take place if and only if $\Gamma > 1.95$ [11]. For $\sigma_0 = -0.05 \text{ C m}^{-2}$, $\Gamma \approx 1.9$, which is just of this order. Our results are in agreement with these calculations since charge reversal is found for -0.05 C m^{-2} but not for -0.02 C m^{-2} , as mentioned before.

The results corresponding to $\sigma_0 = -0.08 \text{ C m}^{-2}$ are shown in figures 3(a) and (b) ($d = 0.8$ and 0.4 nm, respectively). The differences between them have become minor and the estimates of reversal concentration are quite similar (2 and 3 mM for 0.8 and 0.4 nm, respectively). This obviously suggests that, for this surface charge density, ion size correlations are not the dominant driving force for the charge reversal observed in $\sigma(z)$.

Following this procedure, we can obtain estimates of reversal concentrations for other surface charge densities. In figures 4 and 5, the $\sigma(z)$ functions for a few 3:1 electrolyte concentrations around the reversal point are plotted for $\sigma_0 = -0.11$ and -0.14 C m^{-2} , respectively, and for the ionic diameters previously studied: 0.8 and 0.4 nm ((a) and (b) in each figure). As can be concluded, the results obtained for the two ion sizes are very similar. In fact, the estimated

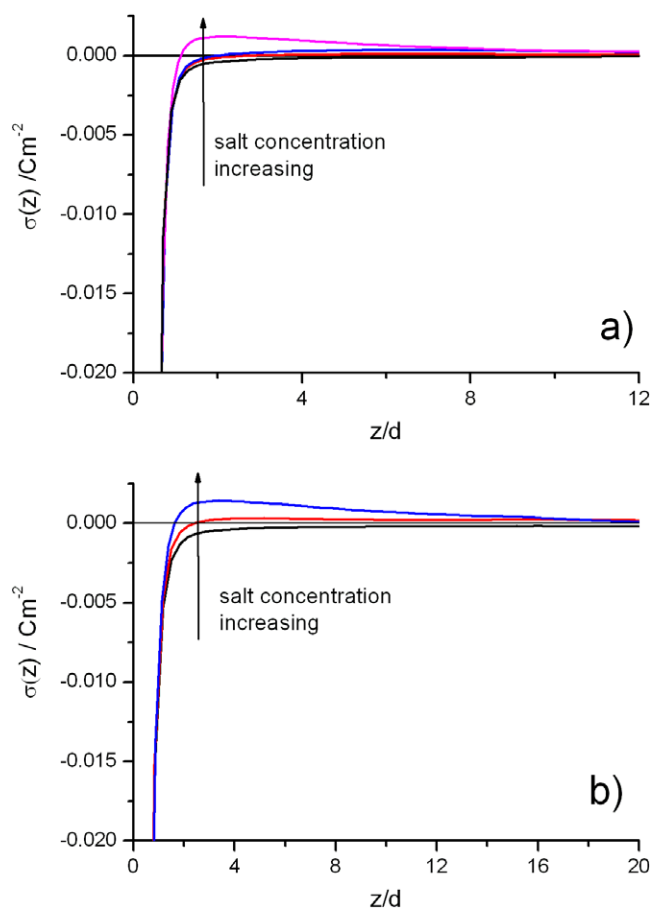


Figure 5. Integrated surface charge density, $\sigma(z)$, for $\sigma_0 = -0.14 \text{ C m}^{-2}$ and (a) $d = 0.8 \text{ nm}$ and 3:1 electrolyte concentrations of 0.5, 1 and 2 mM; (b) $d = 0.4 \text{ nm}$ and 3:1 electrolyte concentrations of 0.4, 0.5, 1 and 2 mM. The electrolyte concentration increases from bottom to top (see the arrow).

reversal concentrations are identical (within the computational uncertainty).

In figure 6, we have summarized all these results plotting the reversal concentration as a function of the surface charge density. As can be seen, the reversal concentration decreases with the absolute value of σ_0 . This is just what the charge reversal models based on strong electrostatic correlations predict. In any case, the differences between these two sizes are important for small surface charge densities but become almost non-existent with increasing this parameter.

Finally it is worth comparing with the inversion curve reported by Diehl and Levin (critical charge density as a function of the salt concentration). These authors concluded that the ion size has a considerable effect on this curve, which apparently disagrees with our results. However, one should bear in mind that they estimated σ_c from the ζ -potential, whose definition straightforwardly involves the ionic size. In other words, in modifying the ionic size, the zeta potential is evaluated at different positions. Thus this property will change regardless of ion size correlations. In fact, the change in ζ due to being evaluated at different positions could be considerably larger than the change associated with ion size correlations and, in any case, one might hardly discriminate these two effects.

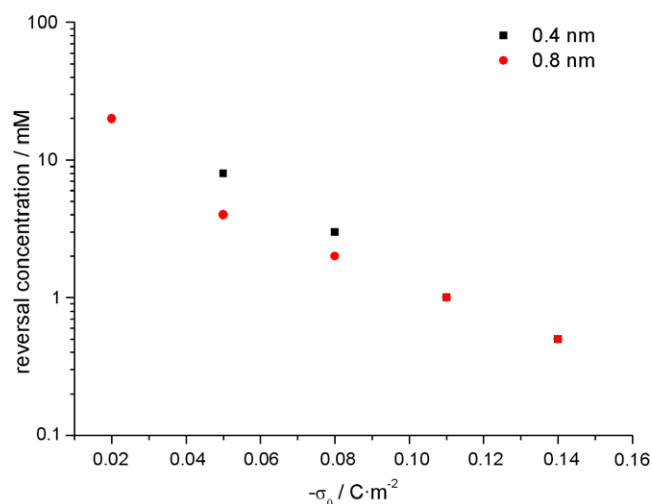


Figure 6. Approximate reversal concentration as a function of the surface charge density for $d = 0.4 \text{ nm}$ (squares) and $d = 0.8 \text{ nm}$ (circles).

In addition, their study is restricted to $|\sigma_0| < 0.08 \text{ C m}^{-2}$ [37]. For such range we have also reported some differences between the results obtained for the two ionic radii studied.

4. Conclusions

In this work we have investigated the effect of ion size correlations on charge reversal (in presence of 3:1 electrolytes) characterizing this phenomenon through the change of behavior of the integrated charge. Our simulations reveal that the strong electrostatic correlations are the dominant mechanism of charge reversal in the case of moderate and large surface charge densities. However, ion size correlations can become crucial at low surface charge densities.

Acknowledgments

The authors are grateful to ‘Ministerio de Educación y Ciencia, Plan Nacional de Investigación, Desarrollo e Innovación Tecnológica (I + D + i)’, projects MAT2006-12918-C05-01 and MAT2006-12918-C05-02, ‘Consejería de Innovación, Ciencia y Empresa de la Junta de Andalucía’, projects P07-FQM-02496 and P07-FQM-02517, as well as the European Regional Development Fund (ERDF), for financial support. AMM also thanks the ‘Programa Ramón y Cajal, 2005, Ministerio de Educación y Ciencia—Fondo Social Europeo’ (RYC-2005-000829).

References

- [1] Grochowski P and Trylska J 2007 *Biopolymers* **89** 93
- [2] Attard P 2001 *Curr. Opin. Colloid Interface Sci.* **6** 366
- [3] Levin Y 2002 *Rep. Prog. Phys.* **65** 1577
- [4] Quesada-Pérez M, González-Tovar E, Martín-Molina A, Lozada-Cassou M and Hidalgo-Álvarez R 2003 *ChemPhysChem* **4** 234
- [5] Fawcett W R 2004 *Liquids, Solutions, and Interfaces* (Oxford: Oxford University Press) chapter 10

- [6] Lyklema J 2006 *Colloids Surf. A* **291** 3
- [7] Guerrero-García G I, González-Tovar E, Lozada-Cassou M and Guevara-Rodríguez F de J 2005 *J. Chem. Phys.* **123** 034703
- [8] Ke W, Yang-Xin Y, Guang-Hua G and Guang-Sheng L 2005 *J. Chem. Phys.* **123** 234904
- [9] Besteman K, van Eijk K and Lemay S G 2007 *Nat. Phys.* **3** 641
- [10] Rodríguez-Pulido A, Martín-Molina A, Rodríguez-Beas C, Llorca O, Aicart E and Junquera E 2009 *Soft Matter* at press
- [11] Pianegonda S, Barbosa M C and Levin Y 2005 *Europhys. Lett.* **71** 831
- [12] Bhuiyan L B and Outhwaite C W 2009 *J. Colloid Interface Sci.* **331** 543
- [13] Netz R R and Orland H 2000 *Eur. Phys. J. E* **1** 67
- [14] Moreira A G and Netz R R 2002 *Eur. Phys. J. E* **8** 33
- [15] Yang-Xin Y, Jianzhong W and Guang-Hua G 2004 *J. Chem. Phys.* **120** 7223
- [16] Gillespie D, Valisko M and Boda D 2005 *J. Phys.: Condens. Matter* **17** 6609
- [17] Grosberg A Y, Nguyen T T and Shklovskii B I 2002 *Rev. Mod. Phys.* **74** 329
- [18] Martín-Molina A, Maroto-Centeno A, Hidalgo-Álvarez R and Quesada-Pérez M 2008 *Colloids Surf. A* **319** 103
- [19] Delville A, Gasmí N, Pellenq R J M, Caillol J M and Van Damme H 1998 *Langmuir* **14** 5077
- [20] Boda D, Fawcett W R, Henderson D and Sokolowski S 2002 *J. Chem. Phys.* **116** 7170
- [21] Valiskó M, Henderson D and Boda D 2004 *J. Phys. Chem. B* **108** 16548
- [22] Bhuiyan B and Outhwaite C W 2004 *Phys. Chem. Chem. Phys.* **6** 3467
- [23] Quesada-Pérez M, Martín-Molina A and Hidalgo-Álvarez R 2004 *J. Chem. Phys.* **121** 8618
- [24] Quesada-Pérez M, Martín-Molina A and Hidalgo-Álvarez R 2005 *Langmuir* **21** 9231
- [25] Henderson D, Gillespie D, Nagy T and Boda D 2005 *J. Chem. Phys.* **122** 084504
- [26] Taboada-Serrano P, Yiacoumi S and Tsouris C 2005 *J. Chem. Phys.* **123** 054703
- [27] Taboada-Serrano P, Yiacoumi S and Tsouris C 2006 *J. Chem. Phys.* **125** 054716
- [28] Martín-Molina A, Quesada-Pérez M and Hidalgo-Álvarez R 2006 *J. Phys. Chem. B* **110** 1326
- [29] Martín-Molina A, Maroto-Centeno A, Hidalgo-Álvarez R and Quesada-Pérez M 2006 *J. Chem. Phys.* **125** 144906
- [30] Labbez C, Jönsson B, Pochard I, Nonat A and Cabane B 2006 *J. Phys. Chem. B* **110** 9219
- [31] Valiskó M, Boda D and Gillespie D 2007 *J. Phys. Chem. C* **111** 15575
- [32] Lenz O and Holm C 2008 *Eur. Phys. J. E* **26** 191
- [33] Ibarra-Armenta J G, Martín-Molina A and Quesada-Pérez M 2009 *Phys. Chem. Chem. Phys.* **11** 309
- [34] Sennato S, Bordi F and Cametti C 2004 *J. Chem. Phys.* **121** 4936
- [35] Besteman K, Zevenbergen M A G and Lemay S G 2005 *Phys. Rev. E* **72** 061501
- [36] Martín-Molina A, Ibarra-Armenta J G and Quesada-Pérez M 2009 *J. Phys. Chem. B* **113** 2414
- [37] Diehl A and Levin Y 2008 *J. Chem. Phys.* **129** 124506
- [38] Diehl A and Levin Y 2006 *J. Chem. Phys.* **125** 054902
- [39] Martín-Molina A, Quesada-Pérez M, Galisteo-González F and Hidalgo-Álvarez R 2003 *Colloids Surf. A* **222** 155
- [40] Israelachvili J 1992 *Intermolecular and Surface Forces* 2nd edn (London: Academic)
- [41] Ottewill R H and Shaw J N 1968 *J. Colloid Interface Sci.* **26** 110
- [42] Elimelech M and O'Melia C R 1990 *Colloids Surf.* **44** 165
- [43] Grahame D C 1947 *Chem. Rev.* **41** 441
- [44] Deserno M, Jiménez-Ángeles F, Holm C and Lozada-Cassou M 2001 *J. Phys. Chem. B* **105** 10983
- [45] Messina R, González-Tovar E, Lozada-Cassou M and Holm C 2002 *Europhys. Lett.* **60** 383
- [46] Madurga S, Martín-Molina A, Vilaseca E, Mas F and Quesada-Pérez M 2007 *J. Chem. Phys.* **126** 234703
- [47] Martín-Molina A, Calero C, Faraudo J, Quesada-Pérez M, Travesset A and Hidalgo-Álvarez R 2009 *Soft Matter* **5** 1350